Results in Engineering 29 (2026) 109674

Contents lists available at ScienceDirect

Results in Engineering

journal homepage: www.sciencedirect.com/journal/results-in-engineering

Research paper

Advanced combustion strategies for enhanced performance and emissions control in light-duty hydrogen internal combustion engines

S. Molina [a], J. Gomez-Soriano [a,*], J.D. Echavarria [a], M. Olcina-Girona [a], D. Gessaroli [b], F.C. Pesce [b]

[a] CMT – Clean Mobility & Thermofluids, Universitat Politècnica de València, Camino de Vera, 46022, Valencia, Spain
[b] Dumarey Automotive Italia S.p.A, Corso Castelfidardo 36, 10129, Torino, Italy

ARTICLE INFO

Keywords:
Hydrogen
Direct injection
Water injection
Lean combustion
Spark-ignition engine

ABSTRACT

This study experimentally investigates combustion and emission control strategies for a spark-ignition direct-injection hydrogen (DI-H_2) engine operating under high-load and high-speed conditions. The work systematically evaluates the influence of air dilution, exhaust gas recirculation (EGR), multi-pulse injection, and water injection on combustion phasing, knock tendency, and cycle-to-cycle variability. Results show that air dilution effectively reduces NO_x emissions-particularly at high excess air ratios ($\lambda \geq 2.2$), while maintaining stable combustion and high efficiency. Advancing combustion phasing toward TDC improves indicated efficiency levels but increases knocking risk at lower dilution levels ($\lambda = 2.0$). EGR dilution, at a fixed $\lambda = 2.3$, further decreases NO_x but leads to unstable operation and reduced gross indicated efficiency (GIE). Multi-pulse injection strategies, in which approximately 20% of the total injected fuel mass is shifted from the main pulse to an early pilot injection during the intake stroke, provide no efficiency gain and increase stability and NO_x compared with single-pulse operation. In contrast, moderate water injection (water-to-hydrogen mass ratio of approximately 2) achieves over 50% NO_x reduction with acceptable combustion stability, while excessive injection (water-to-hydrogen mass ratio of 3) degrades efficiency and stability. Overall, the results highlight air dilution as the most effective strategy for balancing efficiency, emissions, and stability, while water injection offers promising potential for additional NO_x control and knock mitigation. These findings provide quantitative insights into optimizing combustion strategies for high-load DI-H_2 engines and support the development of efficient, low-emission hydrogen combustion systems.

1. Introduction

Hydrogen has gained significant attention as a clean energy carrier due to its potential to drastically reduce greenhouse gas and pollutant emissions compared with conventional fossil fuels [1,2]. It aligns with the European Commission's decarbonization goals for the transport sector, which currently accounts for about 12% of global greenhouse gas emissions [3–6]. However, hydrogen implementation in vehicle propulsion still faces challenges, mainly related to storage, distribution, and material compatibility-high-pressure storage in metallic containers [7,8].

From a combustion standpoint, hydrogen presents both advantages and challenges. Its high calorific value, wide flammability range, and high octane number enable high compression ratios and lean combustion operation. Nevertheless, its low density and high diffusivity require optimized injection and mixture formation strategies to ensure stable combustion and avoid knocking or pre-ignition [9]. Consequently, research has explored a wide range of configurations to exploit these properties. For example, Li et al. [10] proposed and tested a novel concept where hydrogen is directly injected through an aperture on the edge of the spark plug. The results revealed enhanced initial flame propagation and the formation of a stable flame kernel, which substantially extended the lean-burn limit compared to port injection.

In spark-ignition hydrogen engines, the knock limit and combustion stability are key design constraints. Purayil et al. [11] observed that hydrogen enrichment in gasoline engines shortens flame development and propagation durations, improving efficiency but increasing nitrogen oxides emissions (NO_x) at advanced spark timings. Similarly, Naruke et al. [12] demonstrated that moderate hydrogen fractions extend the knock limit and improve indicated efficiency under lean conditions.

For direct-injection hydrogen engines (DI-H_2), several studies have examined the influence of injection timing, pressure, and stratification on knock and abnormal combustion [13,14]. However, most of these works have focused on moderate-load conditions, while fewer studies

* Corresponding author.
E-mail address: jogoso1@mot.upv.es (J. Gomez-Soriano).

https://doi.org/10.1016/j.rineng.2026.109674
Received 6 November 2025; Received in revised form 9 February 2026; Accepted 19 February 2026
Available online 22 February 2026

have investigated abnormal combustion and emission behavior under high-load or wide-open-throttle (WOT) operation [15,16]. Hong et al. [17] showed that retarding the start of injection increases mixture inhomogeneity and helps suppress knock by reducing diffusion time, though the effect is limited by chamber wall temperatures and mixture reactivity near top dead center [18].

To achieve high power density while maintaining low emissions, researchers have explored multiple dilution and combustion control strategies. Air dilution has been shown to improve efficiency and reduce NO_x by increasing the air-fuel ratio [19], while exhaust gas recirculation (EGR) provides thermal benefits but may compromise combustion stability at high loads. Water injection (WI), on the other hand, offers the potential to reduce NO_x emissions and knocking tendency while alleviating the boost pressure requirements associated with air dilution [20]. Nonetheless, the interactions between these strategies, especially under high-load DI-H_2 operation, remain poorly characterized.

Complementary approaches, such as Variable Valve Timing (VVT), have also been investigated to modulate residual gas fraction and improve efficiency across the load range [21–23]. While such strategies can substitute EGR under certain conditions, their combined effect with hydrogen direct injection and dilution control requires further study.

In summary, the literature reveals substantial progress in understanding hydrogen combustion and emission control mechanisms; however, a clear gap persists regarding the comparative assessment of air dilution, EGR, multi-pulse injection, and water injection strategies under high-load, high-speed DI-H_2 engine operation.

1.1. Contribution and objectives

This study presents an experimental investigation of advanced combustion control strategies for a spark-ignition direct-injection hydrogen (DI-H_2) engine operating under high-load conditions. The main objective is to characterize how different dilution and injection strategies affect combustion behavior, efficiency, and emission formation in high-power regimes, which are critical for realizing competitive hydrogen-based propulsion systems.

While previous research by the authors and others has addressed aspects such as air or EGR dilution, variable valve timing, and numerical modeling of hydrogen combustion under moderate load conditions [19–21], the present work extends this knowledge by providing a comprehensive experimental comparison of four key strategies (air dilution, EGR, multi-pulse injection, and water injection) specifically under high-load and high-speed operation. This combination of conditions and control methods has not been jointly analyzed before.

The specific contributions of this work are as follows:

- A systematic experimental evaluation of hydrogen DI combustion under varying dilution mechanisms (air, EGR, and their combination), identifying stability and emission thresholds at λ levels up to 2.3.
- An analysis of multi-pulse injection strategies, in which a pilot pulse (20% of total injected mass) is introduced during the intake stroke, quantifying its effects on mixture formation, combustion variability, and NO_x emissions.
- An assessment of water injection as a knock-mitigation and NO_x-reduction technique, including the identification of optimal water-to-hydrogen ratios for stable operation.

Compared with previous investigations, this study advances beyond previous experimental and simulation works by integrating and comparing multiple combustion strategies within a unified experimental framework under severe (maximum load and high-speeds) operation, enabling a direct assessment of trade-offs among efficiency, stability, and emissions. The results provide new insights into the control of DI-H_2 combustion and contribute to defining practical pathways for efficient and clean hydrogen-fueled engines.

Table 1
Main engine specifications.

Number of cylinders	1
Number of strokes	4
Displaced volume	489.1 cm^3
Stroke	90.4 mm
Injection systems	DI
Ignition system	Spark (Spark plug)
Cylinder diameter	83.0 mm
Compression ratio	12
Connecting rod length	145.0 mm
Valves per cylinder	2 intake, 2 exhaust

2. Materials and methods

This section outlines the tools and methods employed in the investigation, providing a clear and concise overview of the experimental techniques and procedures.

2.1. Experimental tools

The experimental measurements were conducted on a single-cylinder spark ignition (SI) direct injection (DI) engine, which is based on a diesel engine platform. The main engine specifications are provided in Table 1.

The engine was installed in a test cell equipped with various state-of-the-art measurement devices. Fig. 1 illustrates the test cell arrangement, indicating the locations for pressure and temperature measurements, fuel injection, and other relevant devices.

The intake pressure and temperature were controlled using an external compressor, an air conditioning system. The desired exhaust back pressure was set using a knife-gate valve. Table 2 describes the auxiliary systems, while Table 3 details the accuracy of the gas analyzer [19].

It is important to note that since the engine is not equipped with a turbocharger, a knife-gate valve was used to control the back pressure by adjusting the opening percentage and simulating the presence of a turbocharger. The back pressure is calculated using a 0D model, which uses as input parameters engine speed, fuel mass flow, air mass flow, inlet manifold pressure, and inlet and exhaust temperatures.

The hydrogen supply line consisted of pressurized tanks for storage, a pressure discharge control system, and an injector. The injector used in this setup was a prototype designed for gaseous fuels. The water injection system included an air-water tank pressurized at 5 bar, a pressure reducer for the compressed air at 8 bar, which feeds into the tank, and a flow meter at the tank outlet. The water injector was a Bosch injection valve EV 14 0280.158.040 with a flow rate of 0.67 L/min, typically used in gasoline engines.

To record the experimental data, the online combustion diagnostic software (INDICOM) was installed on the test cell, allowing for real-time monitoring and acquisition of key in-cylinder parameters such as Indicated Mean Effective Pressure (IMEP), Heat Release Rate (HRR), and combustion phasing (mas fuel burnt, MFB_{50}). Cycle-to-cycle variability was evaluated through the coefficient of variation of IMEP (COV_{IMEP}).

In-cylinder pressure data were measured using a high-frequency piezoelectric transducer Kistler 6125C, and crank-angle synchronization was achieved with an optical encoder providing an angular resolution of 0.5 crank angle. Data acquisition was performed at a sampling rate of 180 kHz, ensuring accurate representation of in-cylinder pressure fluctuations.

Additional tools were used, including piezoresistive pressure sensors for measuring average flow pressures, a Yokogawa digital YEWFLO vortex flow meter (DY040 S2) for air mass flow measurement, and a Bronkhorst F-203AV-M0-AGD-55-V for hydrogen mass flow measurement. The emissions from the combustion process were analyzed using a HORIBA MEXA-7100DEGR gas analyzer.

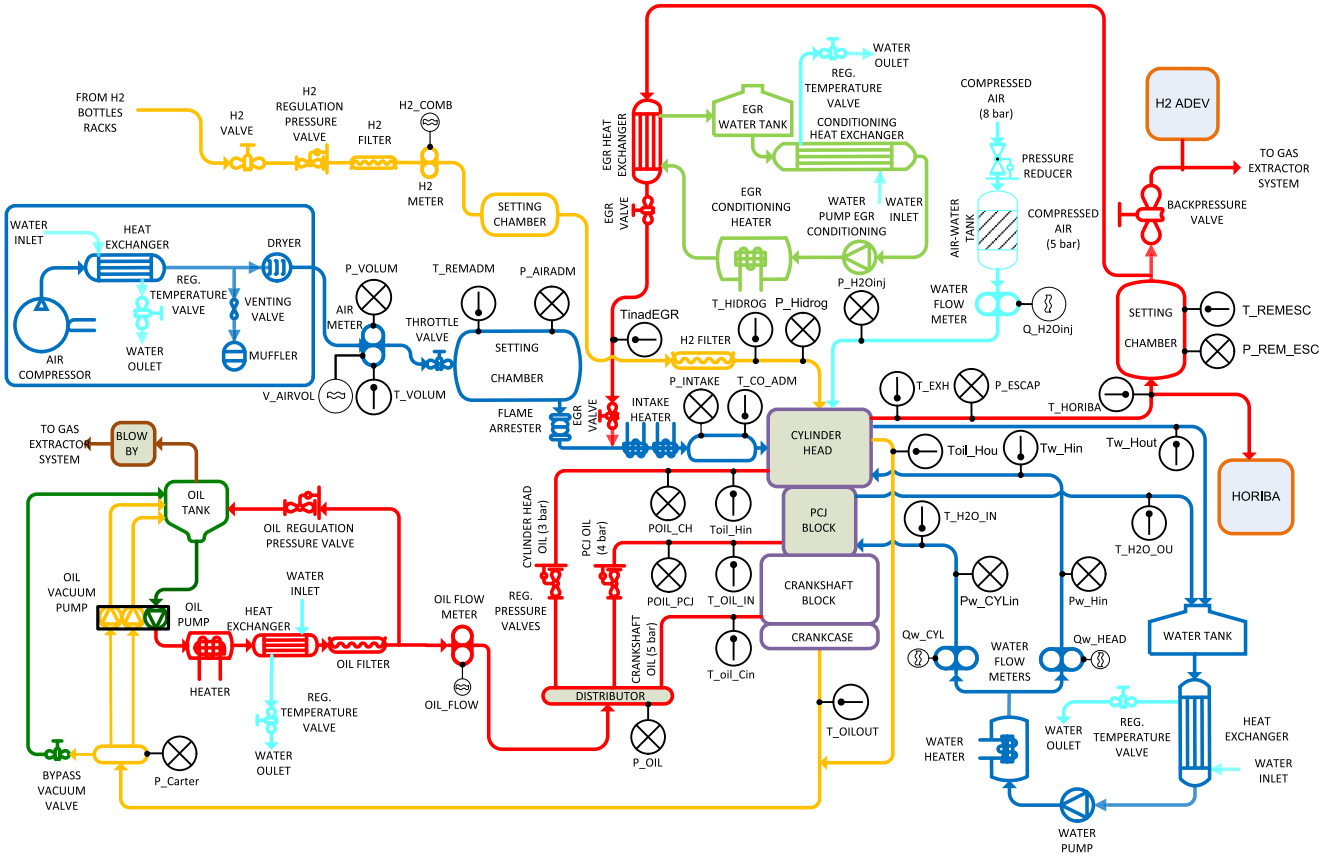

Fig. 1. Experimental engine layout.

Table 2
Accuracy of the test cell instrumentation.

Variable measured	Device	Manufacturer/model	Range/Accuracy
In-cylinder pressure	Piezoelectric transducer	Kistler / 6125C	0–300 bar / ±0.4% linearity
Intake pressure	Piezoresistive transducer	Kistler / 4045A	0–5 bar /±0.3% linearity
Exhaust pressure	Piezoresistive transducer	Kistler / 4049B05	0–5 bar /±0.3% linearity
Temperature in flow pipes	Thermocouple	TC direct / type K	0–1000 °C / ±0.5 °C
Crank angle, engine speed	Encoder	AVL / 365	0–20000 rpm / ±0.5 CAD
NO_x, O_2, CO_2	Gas analyzer	HORIBA / MEXA 7100 DEGR	- / ±1%
Hydrogen mass flow	Fuel balences	Bronkhorst / F-203AV-M0-AGD-55-V	33–1670 l_n/min / ±0.5%
Air mass flow	Air flow meter	YOKOGAWA / DY040 S2	21.8–9153 Nm^3/h / ±1%

Table 3
Accuracy levels of HORIBA MEXA 7100 DEGR for measurements of gaseous pollutants.

Pollutant	Analyzer	Range	Accuracy
HC	FID	min. 0 to 10 ppm C max. 0 to 50 kppm C	± 1%
NO_x	CLD	min. 0 to 10 ppm max. 0 to 10 kppm C	± 1%
CO	NDIR	min. 0 to 3 kppm C max. 0 to 12 vol%	± 1%
CO_2	NDIR	min. 0 to 5 kppm C max. 0 to 20 vol%	± 1%
O_2	PMA	min. 0 to 5 vol% max. 0 to 25 vol%	± 1%

For each operating point, 200 consecutive cycles were recorded. This number of cycles represents a reasonable compromise between ensuring statistical stability of the measurements and limiting data storage and processing requirements. Moreover, it falls within the typical range adopted in similar experimental studies (150-500 cycles), providing sufficient accuracy for averaging and subsequent thermodynamic analysis. Furthermore, each operating condition was measured three times to confirm the repeatability of the results, with the variability between repetitions shown as error bars in all figures.

The raw pressure data were filtered using a low-pass Butterworth filter with a cutoff frequency of 4 kHz to remove high-frequency noise before performing the heat release analysis. The apparent heat release rate (HRR) was calculated using the first law of thermodynamics, assuming a single-zone model with variable specific heats. Post-processing of the recorded data and statistical averaging were carried out using MATLAB routines developed in-house to determine mean pressure traces, HRR profiles, and combustion phasing parameters.

2.2. Experimental procedure

The methodology used in this investigation aimed to evaluate the impact of different strategies on combustion, efficiency, engine knocking, and NO_x reduction. The selected operating conditions correspond to an engine speed of 3000 rpm at full load. The choice of 3000 rpm at

wide-open throttle was made to focus on high-load operation representative of peak engine power conditions.

First, air dilution was evaluated using λ values of 2.3, 2.2, and 2.0. This was achieved by varying the injected fuel while keeping the airflow constant. As a result, reducing the air dilution ratio directly increases the amount of injected fuel, and consequently, the engine's power output. Four conditions were assessed for each air-fuel ratio, maintaining a constant SoI at 160 CAD while varying the combustion phasing. The dilution range of 2.0-2.3 was selected to explore realistic air dilution levels that balance performance and knock risk.

Second, exhaust gas recirculation (EGR) was assessed using two approaches. The first approach involved keeping the air-fuel ratio constant at $\lambda = 2.3$ while varying the EGR levels at 0%, 10%, and 15%. The second approach involved varying the air-fuel ratio with values of 2.3, 2.2, and 2.0 by adjusting the hydrogen injection while maintaining a constant 10% EGR. EGR rates of 10% and 15% were selected based on prior studies to evaluate moderate recirculation effects without compromising combustion stability.

The third strategy involved multi-pulse injection to rapidly homogenize the air-fuel mixture. This was done using two injections: one delivering 80% of the fuel and a pilot injection of 20%. The 20% pilot fuel fraction was chosen, following literature recommendations, as a compromise between avoiding excessive compression work and preserving sufficient mixture homogeneity for stable ignition, allowing assessment of its impact on stratification and combustion variability. The reference case, with SoI fixed at 160 CAD, was compared to cases where the pilot injection was advanced to 280, 300, and 320 CAD, while the main injection remained fixed at 160 CAD. The hydrogen injection pressure was kept constant at 30 bar during all operating conditions.

The fourth and final strategy was water injection, aimed at reducing emissions and preventing knocking combustion. In these experiments, water was injected at $SoI_{water} = 200$ CAD, with water-fuel ratios of 1, 2, and 3, while the fuel injection onset remained at 160 CAD with $\lambda = 2.3$. The start of water injection (SoI_{water}) was chosen to ensure that the entire injected mass, especially for the longest injection duration (W3), was delivered before the intake valves closed, allowing complete in-cylinder admission. The water injection pressure was set to 5 bar.

3. Results and discussion

This section is divided into four subsections, each corresponding to the combustion strategy analyzed. The results focus on three main aspects of hydrogen combustion engines: efficiency and performance, NO_x emissions, and abnormal combustion phenomena that could limit the operation range of these engines.

3.1. Effects of air dilution

The first strategy focuses on studying the effect of air dilution on the combustion and efficiency of the hydrogen engine. Hydrogen's properties allow for stable combustion at high dilution ratios ($\lambda > 2$), a technique thoroughly explored in the literature, with well-documented benefits. Air dilution helps reduce combustion chamber temperatures, which mitigates adverse effects such as increased wall heat losses or NO_x emissions. It is widely acknowledged that NO_x emissions decrease significantly when the air-fuel mixture reaches a dilution level of $\lambda = 2$.

The impact of dilution on NO_x emissions shows a marked reduction across different lambda values. In Bao et al. study [24], distinct zones were defined to represent the dominant NO_x formation mechanisms.This work demonstrates that most operating conditions fall within the region where the thermal mechanism is most dominant. Therefore, selecting the air-to-fuel ratio requires balancing the reduction of NO_x emissions with maintaining high power output. In this study, we focus on three different levels of air dilution, namely $\lambda = 2.3$, 2.2, and 2.0. To modify the dilution ratio, the amount of injected fuel is varied while keeping the air quantity constant, so reducing the air dilution ratio directly increases the injected fuel and, consequently, the engine power output.

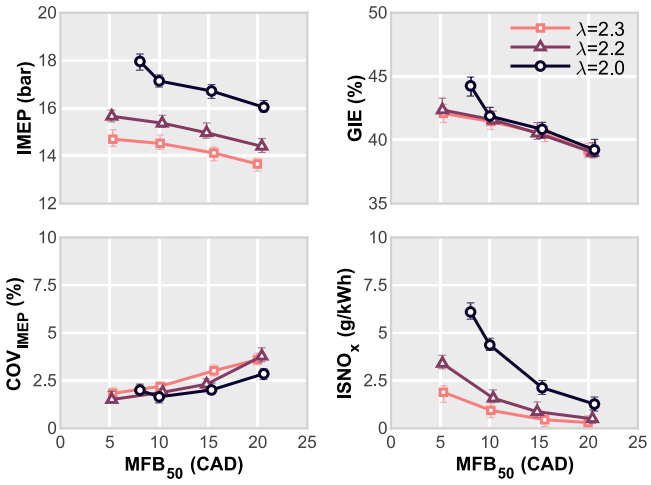

Fig. 2. Performance (IMEP, GIE (Gross Indicated Efficiency) and COV_{IMEP}) and NO_x (specific) emissions results across different air-to-fuel ratios.

The onset of injection was fixed at -160 CAD relative to the Top Dead Center (TDC) of the firing cycle for all air-to-fuel ratio conditions. At this point, the intake valves are already closed, preventing volumetric efficiency losses due to the low density of hydrogen. Additionally, this timing is sufficiently far from the start of combustion to ensure a uniform air-fuel mixture, maintaining combustion stability. The balance between advancing and delaying injection for optimal volumetric and thermal efficiency has been thoroughly analyzed by Molina et al. [25]. This is particularly critical at high loads and engine speeds, where the large amount of injected fuel results in an injection duration that can occupy a third to half of the compression stroke. Under these conditions, backfire is prevented since hydrogen is injected after Intake Valve Closing (IVC); however, pre-ignition and end-gas knocking may still occur.

Fig. 2 shows the results for IMEP, GIE, COV_{IMEP}, and NO_x emissions. As expected, IMEP increases as the λ value decreases due to the increased fuel input. The GIE remains nearly identical for the same air-to-fuel ratio and combustion phasing. Gains in GIE when the combustion phasing is moved toward TDC are approximately 2% across all air-to-fuel ratios considered. This improvement is attributed to a reduction in heat losses and a higher effective expansion ratio when combustion occurs closer to TDC, which enhances thermodynamic efficiency. Combustion stability is also similar, with a higher COV_{IMEP} observed for higher air-to-fuel ratio values ($\lambda = 2.3$ and 2.2), particularly with more delayed combustion phasing. Similar efficiency gains with advanced phasing have been reported by Novella et al. [19].

Regarding NO_x emissions, a reduction is observed as the λ value increases, with the effect becoming more pronounced as the combustion phasing approaches TDC. In addition, Fig. 2 shows that combustion phasing has a more significant effect on efficiency and NO_x emissions than the λ value. Performance improves as combustion phasing approaches TDC, leading to higher IMEP and GIE. Combustion stability is also noticeably enhanced, as indicated by the COV_{IMEP} results. The reduction trends observed in this study are consistent with those reported by Bao et al. [24], who identified a similar shift from prompt to thermal NO formation mechanisms above $\lambda = 2$. In both studies, the suppression of NO_x correlates with the decrease in peak flame temperature and oxygen availability.

It is important to note that measurements for the $\lambda = 2.0$ condition with a MFB_{50} located at 5 CAD are not feasible due to knocking appearance. The slight increase observed in the IMEP and GIE graphs in Fig. 2 are attributed to the occurrence of end-gas auto-ignition.

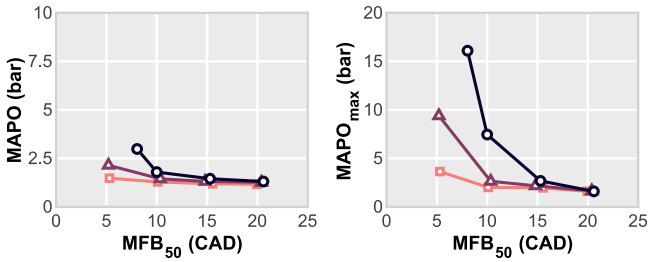

Fig. 3. Analysis of knocking appearance. Cycle average and maximum MAPO levels at different levels of air dilution ratio.

To deepen the analysis of this phenomenon, the Maximum Amplitude Pressure Oscillation (MAPO) parameter was computed for each recorded cycle and is presented in Fig. 3, along with the cycle average and maximum values. An increase in the mean MAPO is observed as combustion phasing advances, indicating a higher incidence of knocking. This trend aligns with classical knock behavior, as earlier combustion phasing increases in-cylinder pressure and temperature during the end-gas reaction phase, promoting auto-ignition. Comparable findings were reported by Hong et al. [17], who linked the onset of knock under similar λ conditions to elevated end-gas reactivity. Additionally, conditions with higher dilution tend to mitigate this trend, allowing measurements to be closer to a 5 CAD of MFB_{50} compared to lower λ values, where pressure oscillations are more pronounced. This trend is also evident in the maximum MAPO levels. Therefore, the intensification of knocking is significantly influenced by both the precise combustion phasing and the λ values.

In Fig. 4, the distribution of MAPO levels for each cycle during some specific tests is examined, alongside the monitoring of in-cylinder pressure during the cycle with the highest MAPO level (the one highlighted by a red dashed circle). The top graphs correspond to a $\lambda = 2.0$ condition with varying MFB_{50} values. The bottom graphs, on the other hand, show MAPO levels for different λ values with an MFB_{50} of 5 CAD. The aim is to gain insight into potential knocking occurrences, even in cases where it should not be a problem on average.

It is observed that advancing combustion timing increases both the frequency and intensity of knocking, as shown in Fig. 3. This effect becomes particularly pronounced when the combustion phasing reaches MFB_{50} at 10 CAD. Additionally, the effects of altering λ values on knocking reduction are less significant compared to the influence of combustion phasing. Below a λ value of 2.2, there is a notable increase in knocking, with a λ value of 2.3 being the only value that manages to keep knocking within acceptable limits.

To mitigate knocking in conditions prone to it, retarding the combustion phasing is recommended as a viable strategy. This approach helps prevent the occurrence of this abnormal combustion phenomenon, particularly in high-power scenarios where a large volume of air is required due to a combination of high λ values and increased fuel demand. Such conditions can pose challenges for turbochargers or supercharging systems. However, it is important to note that this strategy may lead to performance losses, as illustrated in Fig. 2, and could negatively impact overall fuel consumption under these conditions. These findings highlight the well-known trade-off between knock suppression and thermal efficiency, consistent with prior analyses of hydrogen DI engines [26]. The results confirm that optimizing combustion phasing near the knock limit remains essential to balance performance and durability under high-load operation.

3.2. Effects of EGR dilution

Exhaust gas recirculation (EGR) is a widely adopted technique in internal combustion engines, primarily aimed at reducing NO_x emissions. This method involves the controlled reintroduction of a portion of the engine exhaust gases back into the combustion chamber. While EGR is most commonly associated with gasoline and diesel engines, it is also applicable to hydrogen combustion engines. In this section, we will conduct a detailed examination of the impact of high levels of EGR on NO_x emissions, engine performance, and susceptibility to knocking combustion. To assess the effectiveness of EGR, we have measured oxygen levels from both intake and exhaust sources, as outlined in the following equation from Verhelst et al. [27]:

$$EGR(\%) = \frac{O_2^{atm} - O_2^{adm}}{O_2^{atm} - O_2^{exh}} \cdot 100 \quad (1)$$

High-pressure EGR was studied from two distinct perspectives. First, the effect of varying the EGR rate while keeping the air dilution ratio and air mass flow constant was examined. This involved assessing EGR percentages of 0%, 10%, and 15% at a λ value of 2.3. Second, the impact of increasing λ under a constant EGR condition (10% EGR) was investigated, with λ values varying from 2.3 to 2.2 and 2.0.

3.2.1. Effects of EGR dilution at λ constant

Performance and NO_x emission results for different levels of EGR are a constant λ value of 2.3 are shown in Fig. 5. For the investigation of EGR variation, EGR rates were incrementally increased while maintaining a constant air-fuel ratio, necessitating increases in both boost pressure and exhaust back pressure. As observed, the increase in EGR dilution resulted in reduced stability, particularly as combustion approached TDC. These results show an opposing trend compared to the λ sweep findings, as presented in Fig. 2.

This opposite trend can be explained by the different mechanisms through which EGR and air dilution influence combustion. While air dilution increases the mixture's heat capacity and lowers the adiabatic flame temperature without significantly affecting the oxygen concentration, EGR reintroduces inert exhaust gases that simultaneously decrease oxygen availability and increase the residual gas fraction. This leads to slower flame development, thereby penalizing combustion stability and thermal efficiency.

Considering that a common stability criterion is to keep the COV_{IMEP} below 5%, none of the considered EGR levels are capable to operating at stable regime. The reduced stability led to decreased performance and thermal efficiency (GIE), subsequently shifting the Maximum Brake Torque (MBT) point towards the expansion stroke. Similar reductions in combustion stability with increasing EGR have been reported by Novella et al. [21] and Verhelst [27], confirming that high EGR ratios are generally unsuitable for high-load hydrogen operation.

Regarding NO_x emissions, they decrease with higher EGR ratios, though the impact is less significant compared to the air-to-fuel ratio sweep shown in Fig. 2. Nonetheless, these findings suggest that combining such high EGR dilution levels with lean mixtures (around $\lambda = 2.3$) may not be practical.

3.2.2. Effects of air dilution at EGR constant

In this section, the effect of varying λ at a constant EGR rate of 10% on both performance and NO_x emission levels is analyzed. Fig. 6 illustrates a combustion phasing sweep for each dilution condition. As in the previous sections, the air mass flow rate was kept constant in all cases, meaning that λ was controlled by the hydrogen amount injection.

As expected, the IMEP levels show a stepped pattern with the injected fuel for each case, with lower λ values resulting in higher IMEP levels. It is also observed that the MBT phasing is positioned between MFB_{50} at 10 and 5 CAD, as indicated by the trend change in the $\lambda = 2.2$ and 2.3 cases. In the case of $\lambda = 2$, it is not possible to identify this change in trend because severe knocking conditions were observed when advancing the combustion beyond 10 CAD of MFB_{50}. This behavior agrees with typical hydrogen combustion trends, where advancing phasing improves thermal efficiency up to the knock limit. However, the presence of EGR delays flame propagation and lowers peak in-cylinder

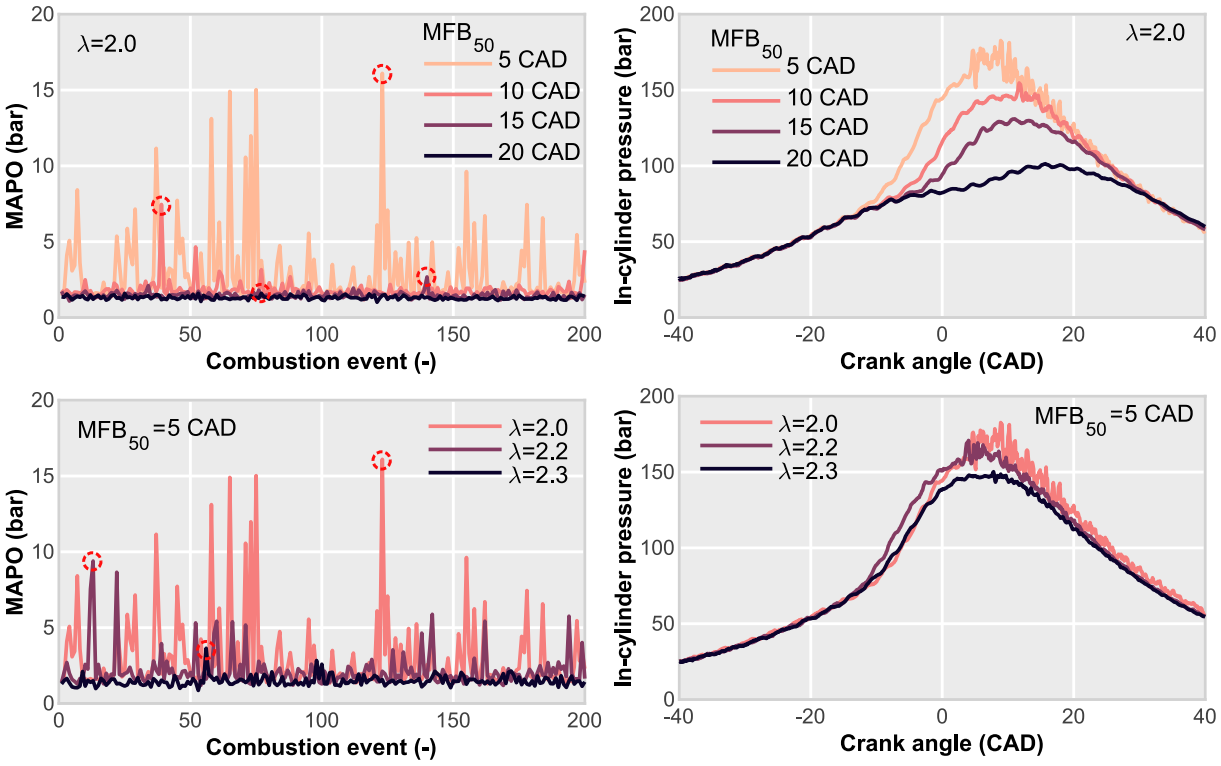

Fig. 4. Analysis of knocking occurrence, including MAPO levels for each recorded cycle and the in-cylinder pressure evolution of the engine cycle with the highest MAPO level.

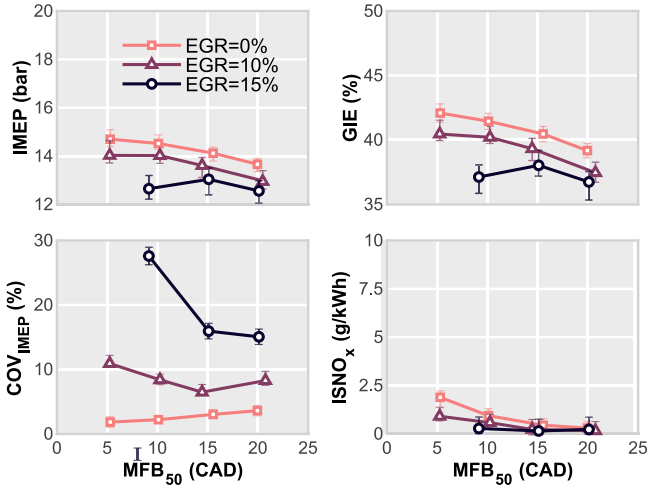

Fig. 5. Performance (IMEP, GIE and COV_{IMEP}) and NO_x (specific) emissions results across different EGR levels at $\lambda = 2.3$.

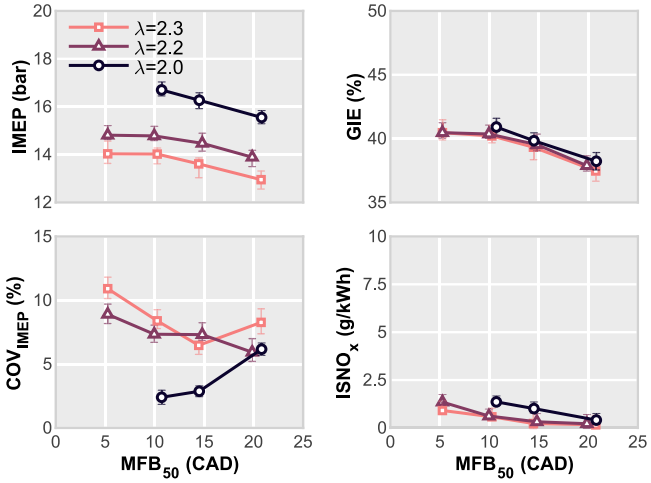

Fig. 6. Performance (IMEP, GIE and COV_{IMEP}) and NO_x (specific) emissions results across different air dilution ratios at 10% of EGR dilution.

temperatures, narrowing the range of stable operation compared to air dilution alone [21].

In terms of efficiency, GIE levels are similar across all dilution conditions, indicating that combustion phasing is the most critical factor for achieving high efficiency under these operating conditions. Maximum efficiency levels of around 41% are observed. Increasing λ does not improve efficiency when combined with moderate EGR levels (10%); in fact, slightly higher efficiency is observed at $\lambda = 2$, likely due to the lower CCV noted in this condition. This can be attributed to the competing effects of increased specific heat capacity (reducing temperature and NO_x) and the slower chemical kinetics introduced by the reduced oxygen fraction from EGR, which limits combustion speed and overall efficiency.

Additionally, increasing λ with a 10% EGR rate appears to generally improve stability without significantly affecting NO_x production compared to the cases shown in Fig. 5. More diluted conditions, such as $\lambda = 2.3$ and 2.2, reduce NO_x by approximately 0.5 g/kWh at MFB_{50} values of 10 and 15 CAD. Under these conditions, CCV decreases but increases near the extreme combustion phasing values (5 and 20 CAD). COV_{IMEP} rises well above 5% in nearly all cases, except at $\lambda = 2$ with an MFB_{50} of 10 and 15 CAD. These observations are consistent with the expected destabilizing effect of EGR at high dilution levels, as also reported by Hong et al. [17], who associated increased residual gas fraction with extended ignition delay and larger cycle-to-cycle variations. The combined influence of reduced oxygen availability and lower flame speed, likely explains the unstable operation observed under these conditions.

3.3. Multi-pulse injection effects

Multi-pulse injection is a technique commonly used in internal combustion engines, particularly in compression ignition (CI) engines. Unlike a single injection scheme, which injects fuel into the combustion chamber once per engine cycle, multi-pulse injection involves multiple events within the same engine cycle.

The primary objective of this approach is to avoid the formation of a heterogeneous air-fuel mixture, which is a significant disadvantage of DI hydrogen engines. It is well known that delaying injection improves efficiency by reducing the compression work [28]. However, this delay increases NO_x emissions, reduces combustion efficiency, and encourages abnormal combustion phenomena such as knocking or pre-ignition, which typically limit the potential benefits of delaying injection.

A pilot injection can reduce mixture heterogeneity in the combustion chamber, enhancing combustion stability. This approach seeks to refine the injection distribution, allowing a shift toward more diluted conditions or a more delayed SoI to improve efficiency. The pilot injection promotes localized turbulence and partially premixed regions that can enhance ignition kernel development in subsequent injections [9]. The timing and mass fraction of the pilot pulse strongly influence the local equivalence ratio and, consequently, the ignition delay and early flame growth.

In this section, the total injected fuel remains consistent with the reference case, but it is distributed across two injections. The main injection occurs after IVC, supplying 80% of the fuel to avoid volumetric efficiency penalties. The remaining 20% is injected as a pilot injection to minimize prolonged exposure to high hydrogen concentrations, reducing the risk of pre-ignition while minimizing volumetric efficiency losses. Fig. 7 illustrates the specific cases under investigation. Three different cases were tested in addition to the baseline, which consists of a λ of 2.3 and no EGR. These strategies are identified by a pair of numbers separated by the "/" character. The first digit corresponds to the start of the main injection in CAD before firing TDC. The second follows the same sequence but for the pilot injection.

Fig. 8 shows the results of all considered multi-pulse injection strategies in terms of performance, combustion stability and specific NO_x. A quick inspection reveals that multi-pulse injection does not contribute to increase the thermal efficiency. Indeed, the proposed multi-pulse strategies exhibit a general decrease of 1.0% in GIE and increased cycle-to-cycle variability (CCV) and NO_x emissions compared to the reference single-injection case. The 160/320 strategy is the only configuration capable of achieving GIE levels similar to the single-injection baseline, though these gains are offset by increased CCV and higher NO_x emissions. Similar trade-offs between efficiency, NO_x, and stability have been reported in studies with gaseous fuels [29], where the increased cycle-to-cycle variability was linked to uneven local equivalence ratios and residual hydrogen pockets. The results in the present work align with these findings, suggesting that the main limitation of multi-pulse injection lies in maintaining uniform mixture conditions during the delay between pulses.

It is difficult to establish a reasonable cause for the increase in COV_{IMEP} when switching to a multi-pulse strategy and its subsequent effects on performance and NO_x emissions with the experimental information available in this study.

However, inspection of the knocking events may help to shed some light on this regard. Fig. 9 shows the cycle average and maximum MAPO levels at the single-pulse case and different multi-pulse injection strategies. As observed, splitting the injection leads to an increased number of knocking events. This effect can explain the rise in COV_{IMEP}, as knocking cycles contribute to this parameter similarly to misfiring cycles. The increase in NO_x emissions can also be attributed to higher local temperatures caused by the auto-ignition of the mixture. However, there is no clear relationship with the expected improvement in mixing conditions by dividing the injection into two pulses.

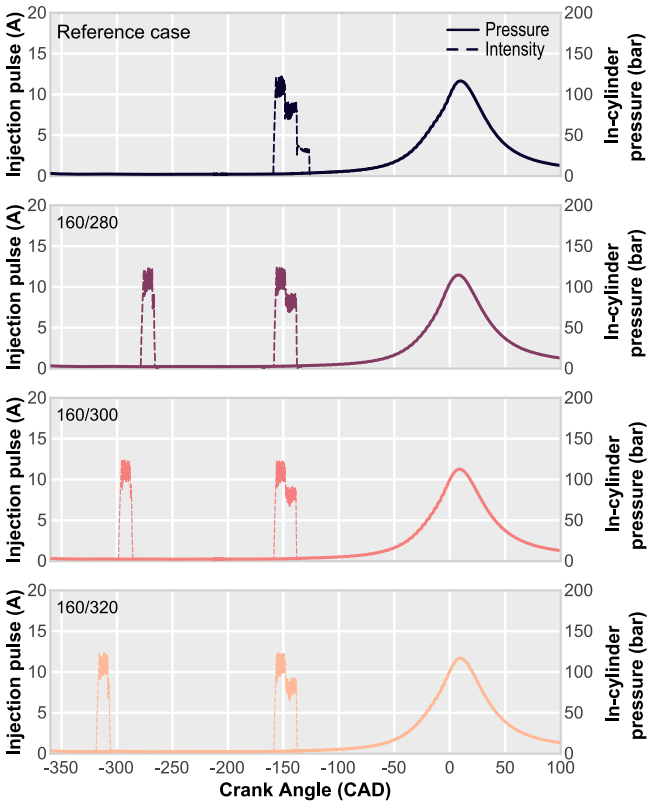

Fig. 7. Multi-pulse injection strategies, showing the spark plug intensity signal alongside in-cylinder pressure to illustrate the distribution of the injected hydrogen.

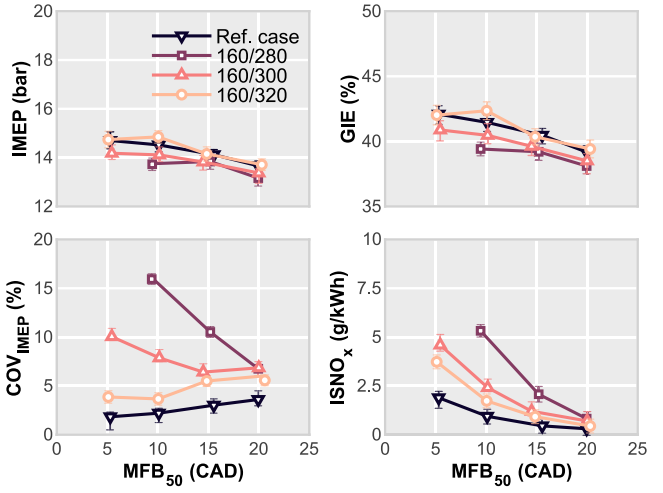

Fig. 8. Performance (IMEP, GIE and COV_{IMEP}) and NO_x (specific) emissions results across different multi-pulse injection strategies.

One would expect that switching to multi-pulse injection would result in a more homogeneous mixture, leading to more stable combustion and lower CCV during engine operation. Additionally, it is possible that part of the observed increase in COV_{IMEP} arises from the decay of turbulence caused by splitting the injection. The time delay and separation between pulses may reduce the turbulence intensity generated by the pilot injection before the main injection occurs, potentially leading to less efficient mixture entrainment and local inhomogeneities. While this effect cannot be directly quantified with the current experimental setup, it represents a plausible mechanism contributing to the increased cycle-to-cycle variability observed in the multi-pulse strategies. Future

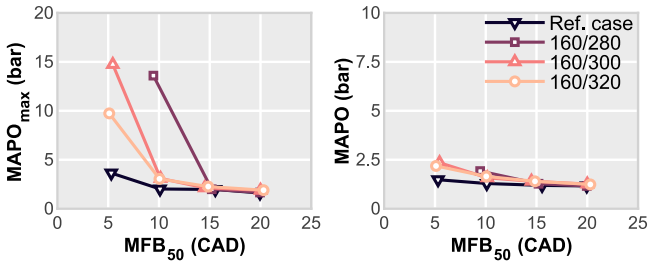

Fig. 9. Analysis of knocking appearance. Cycle average and maximum MAPO levels at different multi-pulse injection strategies.

studies employing optical diagnostics or high-fidelity numerical simulations could provide further insight into the role of turbulence decay in mixture formation under these injection schemes.

The observed increase in COV_{IMEP} may also be related to the decay of turbulence and vorticity between injection events. The time separation between the pilot and main injections allows part of the turbulent kinetic energy generated by the pilot jet to dissipate before the main injection begins, reducing local mixing intensity and increasing stratification gradients. This mechanism has been previously suggested by Xie et al. [13] as a key factor influencing cycle-to-cycle variation in gaseous direct injection engines.

Instead, multi-pulse injection seems to excessively lean the mixture, potentially leading to misfire cycles followed by a knocking cycle due to the higher concentration of unburned H_2 from the previous cycle. This reasoning cannot be fully validated with the available results due to the limitations of the experimental techniques used in this study. Further research is necessary in this area, utilizing optical techniques or numerical methods to gain a deeper understanding of mixture formation in this engine.

3.4. Impact of water injection

Water injection has emerged as a promising technique for hydrogen-fueled engines, particularly in PFI configurations, effectively addressing key challenges such as limited volumetric efficiency and high NO_x emissions. By leveraging the latent heat of vaporization and the endothermic properties of water, this method helps suppress NO_x emissions. As water transitions from liquid to vapor, it absorbs heat from the surrounding air-fuel mixture, thereby lowering the overall temperature. Similar cooling and dilution effects have been reported in hydrogen and natural-gas-fueled engines [20], where water injection significantly lowers in-cylinder temperatures and suppresses thermal NO formation.

This section examines the impact of water injection on engine performance metrics and emissions reduction, with a focus on NO_x. Water injection was conducted into the intake manifold at a constant SOI_{H_2O} of -200 CAD relative to the firing TDC and considering a λ value of 2.3. Three different amounts of water were considered, expressed as ratios to the amount of hydrogen injected, as shown in Eq. (2):

$$W_i = \frac{H_2O^{inj}}{H_2^{inj}} \tag{2}$$

The three cases are identified as follows: $W_1 = 1$, $W_2 = 2$, and $W_3 = 3$.

In Fig. 10, it is observed that adding small amounts of water (between W_1 and W_2) maintains similar levels of GIE compared to the baseline. However, further increasing the water injection to W_3 may result in significant efficiency losses. The efficiency reduction observed at high water fractions is mainly attributed to the lower in-cylinder temperature and slower flame propagation, which extend the combustion duration and reduce the effective expansion work.

The results demonstrate that water injection is an effective method for reducing NO_x emissions. A significant reduction is observed, with

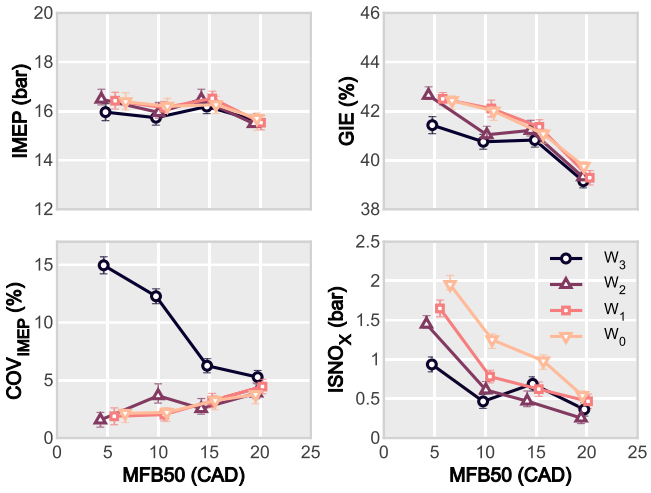

Fig. 10. Performance (IMEP, GIE and COV_{IMEP}) and NO_x (specific) emissions results across different different amounts of water injection.

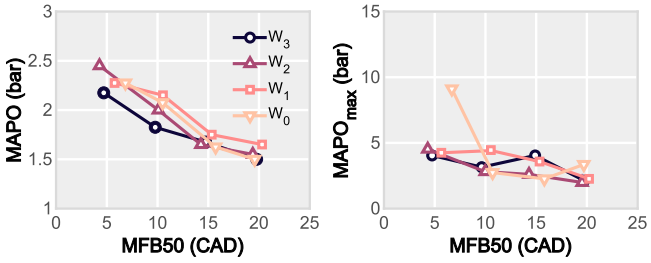

Fig. 11. Analysis of knocking appearance. Cycle average and maximum MAPO levels at different water injection amounts.

decreases of up to 35% at W_1 and over 50% at W_2 for combustion phasing at MFB_{50} = 10 and 15 CAD. Although the reduction of specific NO_x emissions ($ISNO_x$) at MFB_{50} = 20 CAD is not as pronounced due to delayed combustion phasing conditions, the water injection still has a slight mitigating effect on NO_x emissions.

To quantify the impact of water injection on knocking mitigation, the cycle average and maximum MAPO levels are presented in Fig. 11. Although relevant knocking cycles are evident in the $MAPO_{max}$ value of the baseline case with 5 CAD of MFB_{50}, the average value remains too low to be considered a critical condition. As a result, the impact of water injection is somewhat obscured. While an overall reduction in knocking trends is observed with water injection, it is not possible to accurately quantify the effect of the injected water amount on knocking mitigation.

Despite this, this technology decouples pressure boosting from dilution, providing a viable solution to the challenges inherent in hydrogen combustion. Further research and development efforts are needed to fully realize the potential of water injection and accelerate its application in production.

Overall, the results confirm that water injection can effectively control NO_x emissions and partially mitigate knock without compromising performance at moderate water-to-fuel ratios. However, excessive injection levels negatively affect thermal efficiency due to overcooling and incomplete vaporization, indicating that optimizing the water fraction and timing is essential for achieving robust and efficient hydrogen combustion.

3.5. Comparative analysis of technologies

In the final stage of this research, a comprehensive analysis was conducted to compare the strategies presented. All points studied were measured under the same air quantity. Each point from the various sweeps

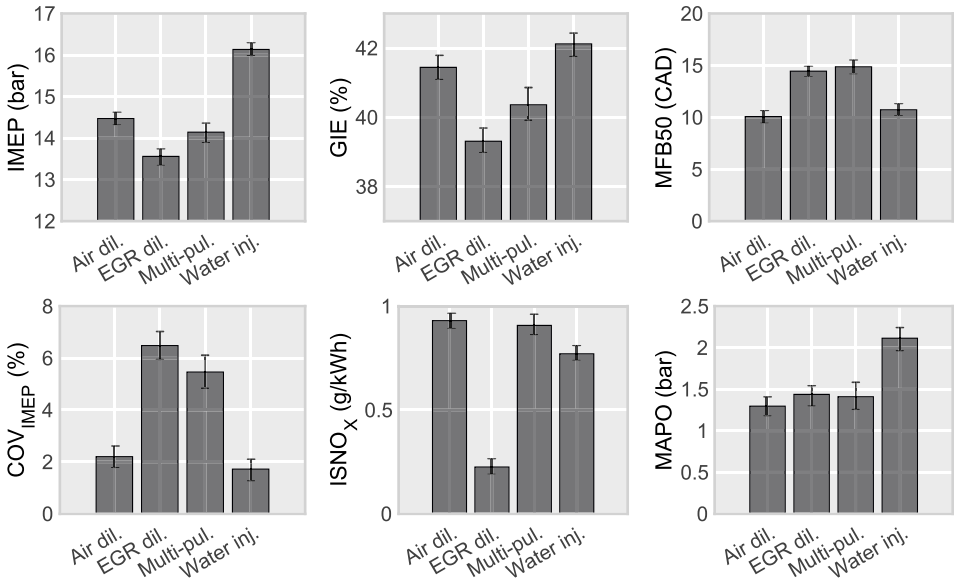

Fig. 12. Comparative analysis of technologies considered in this investigation. IMEP, GIE, COV_{IMEP}, MAPO, $ISNO_x$ and MFB_{50} parameters are sown.

was meticulously evaluated to determine the optimal configuration in terms of efficiency while ensuring that $ISNO_x$ emission levels remained below 1 g/kWh. Additional criteria were also considered, such as maintaining MAPO levels below 3 bar and ensuring combustion stability, with COV_{IMEP} not exceeding 8%. These thresholds were selected to ensure a balanced trade-off between efficiency, combustion stability, and emission control feasibility. The $ISNO_x$ limit of 1 g/kWh was chosen to represent a level compatible with compact aftertreatment systems, while the COV_{IMEP} limit was applied as a practical indicator of acceptable combustion stability (with low hydrogen slip). The MAPO threshold was set to avoid excessively severe knock events, while maintaining safe and repeatable operation. The results of this analysis are presented in Fig. 12, where the most significant engine and combustion parameters are included.

Water injection has been identified as the most effective strategy for enhancing efficiency. It introduces inert gases that are decoupled from the increase in intake pressure while providing a significant cooling effect due to the heat of vaporization of water. This technique enables a higher load with a lower COV_{IMEP}. However, MAPO levels increase by more than 2 bar for every 0.5 bar increase, compared to the other strategies. This can lead to higher in-cylinder pressure as a result of achieving a higher loads.

It is worth noting that both EGR and multi-pulse injection strategies significantly impact combustion stability. The optimal EGR point is the only one that meets the limitation of 8% COV_{IMEP} and is also the most effective method for reducing NO_x emissions. In contrast, the multi-pulse injection shows similar results to those obtained with varying λ, but it exhibits higher CCV.

The use of EGR emerges as an effective method for significantly reducing NO_x emissions. Consequently, exploring various combinations of air dilution and EGR is expected to yield further optimization than what is presented in this study. This highlights the potential for further refinement and enhancement in reducing NO_x emissions through different λ and EGR configurations.

4. Conclusions

This study experimentally investigated advanced combustion strategies for a spark-ignition direct-injection hydrogen (DI-H_2) engine under high-load and high-speed conditions. Based on the results, the following key messages can be drawn:

- Air dilution is the most effective strategy for reducing NO_x emissions while maintaining stable combustion and high efficiency. Careful control of combustion phasing is essential to balance performance and knock risk, particularly at lower excess air ratios ($\lambda \approx 2.0$).
- EGR provides NO_x reduction but compromises stability under high-load conditions, resulting in increased COV_{IMEP} and lower efficiency. Its use should therefore be carefully limited when high power output is required.
- Multi-pulse injection offers limited benefits: redistributing 20% of the fuel mass to a pilot pulse during the intake stroke increases combustion variability and NO_x emissions without improving efficiency.
- Water injection is a promising complementary strategy, capable of reducing NO_x by over 50% at moderate injection levels, while mitigating knocking. Excessive water injection, however, can reduce efficiency and destabilize combustion, indicating the importance of optimizing injection distribution and phasing.
- Integrated strategy assessment is critical: combining dilution, injection, and water strategies provides a pathway to optimize performance, emissions, and stability in high-load DI-H_2 engines. The present findings provide practical guidance for designing control strategies in future hydrogen-fueled combustion systems.

Overall, the study demonstrates that strategic control of combustion and dilution mechanisms under high-load conditions enables hydrogen engines to achieve both high efficiency and low emissions, offering insights that advance the practical application of DI-H_2 technology.

CRediT authorship contribution statement

S. Molina: Writing – review & editing, Funding acquisition, Conceptualization; **J. Gomez-Soriano:** Writing – review & editing, Resources, Methodology, Investigation; **J.D. Echavarria:** Writing – original draft, Visualization, Validation; **M. Olcina-Girona:** Writing – original draft, Visualization, Validation, Investigation; **D. Gessaroli:** Writing – review & editing, Investigation, Conceptualization; **F.C. Pesce:** Writing – review & editing, Resources, Investigation, Funding acquisition.

Funding

This research has been partially funded by Agencia Estatal de Investigación of the Spanish Government through project TED2021-130596B-C21 (BIOH2FUEL).

This research has been partially funded by the “Ayuda a Primeros Proyectos de Investigación” (PAID-06-24), Vicerrectorado de Investigación de la Universitat Politècnica de València UPV.

Data availability

The data that has been used is confidential.

Declaration of competing interest

The authors declare that they have no known competing financial interests or personal relationships that could have appeared to influence the work reported in this paper.

Acknowledgements

The authors wish to thank Mr. Gabriel Alcantarilla and Mr. Daniel Lérida for their inestimable assistance during the experimental campaign.

References

[1] Z. Sun, J. Hong, T. Zhang, B. Sun, B. Yang, L. Lu, L. Li, K. Wu, Hydrogen engine operation strategies: recent progress, industrialization challenges, and perspectives, Int. J. Hydrogen Energy 48 (1) (2023) 366–392. https://doi.org/10.1016/j.ijhydene.2022.09.256

[2] A. Midilli, I. Dincer, Hydrogen as a renewable and sustainable solution in reducing global fossil fuel consumption, Int. J. Hydrogen Energy 33 (16) (2008) 4209–4222. https://doi.org/10.1016/j.ijhydene.2008.05.024

[3] E. Commission, Stepping up Europe’s 2030 climate ambition. Investing in a climate-neutral future for the benefit of our people, 2020, https://scholar.google.com/scholar{_}lookup?title=Stepping+up+Europe’s+2030+climate+ambition+Investing+in+a+climate-neutral+future+for+the+benefit+of+our+people{&}author=European+Commission{&}publication{_}year=2020{&}journal=J.+Chem.+Inf.+Model.{&}volume=53{&}pages=16.

[4] R. Novella, B. Plá, P. Bares, D. Pinto, Online model adaption for energy management in fuel cell electric vehicles (FCEVs), Appl. Sci. 14 (8) (2024) 18. https://doi.org/10.3390/app14083473

[5] H. Ritchie, P. Rosado, M. Roser, CO2 and greenhouse gas emissions: By sector, 2020. https://ourworldindata.org/emissions-by-sector.

[6] M. Granovskii, I. Dincer, M.A. Rosen, Greenhouse gas emissions reduction by use of wind and solar energies for hydrogen and electricity production: economic factors, Int. J. Hydrogen Energy 32 (8) (2007) 927–931. https://doi.org/10.1016/j.ijhydene.2006.09.029

[7] M. Koyama, E. Akiyama, Y.-k. Lee, D. Raabe, K. Tsuzaki, Sciencedirect overview of hydrogen embrittlement in high-Mn steels, Int. J. Hydrogen Energy 42 (17) (2017) 12706–12723. https://doi.org/10.1016/j.ijhydene.2017.02.214

[8] Q. Liu, M. Zhang, Q. Zhou, A. Atrens, A review of hydrogen embrittlement of martensitic advanced high-strength steels 34 (3) (2016) 153–186. https://doi.org/10.1515/corrrev-2016-0006

[9] M. Fischer, S. Sterlepper, S. Pischinger, J. Seibel, U. Kramer, T. Lorenz, Operation principles for hydrogen spark ignited direct injection engines for passenger car applications, Int. J. Hydrogen Energy 47 (8) (2022) 5638–5649. https://doi.org/10.1016/j.ijhydene.2021.11.134

[10] X. Li, Y. Zhuang, Y. Wang, Z. Zhu, Y. Qian, R. Zhai, An experimental investigation on the lean-burn characteristics of a novel hydrogen fueled spark ignition engine: hydrogen injection via a micro-hole on the spark plug, Int. J. Hydrogen Energy 57 (2024) 990–999. https://doi.org/10.1016/j.ijhydene.2024.01.008

[11] S.T.P. Purayil, S.A.B. Al-Omari, E. Elnajjar, Experimental investigation of spark timing on extension of hydrogen knock limit and performance of a hydrogen-gasoline dual-fuel engine, Int. J. Hydrogen Energy 49 (2024) 910–922. https://doi.org/10.1016/j.ijhydene.2023.09.139

[12] M. Naruke, K. Morie, S. Sakaida, K. Tanaka, M. Konno, Effects of hydrogen addition on engine performance in a spark ignition engine with a high compression ratio under lean burn conditions, Int. J. Hydrogen Energy 44 (29) (2019) 15565–15574. https://doi.org/10.1016/j.ijhydene.2019.04.120

[13] F. Xie, Z. Liang, B. Cui, W. Guo, X. Li, B. Jiang, Z. Jin, Spray-to-combustion interaction in hydrogen direct injection engines: effects of injector structure and injection pressure, Energy 333 (C) (2025) 137514.

[14] X. Cai, Z. Wang, J. Yang, S. Wang, C. Ji, H. Wang, H. Meng, H. Li, Effect of injection strategy on a novel hydrogen direct injection stratified combustion rotary engine, Energy 326 (2025) 136125.

[15] Y. Liang, K. Xing, H. Huang, D. Ning, Y. Wang, X. Wang, Investigation of knock combustion mechanism and injection angle optimization in a heavy-duty direct-injection hydrogen engine, Energy 335 (2025) 138041.

[16] X.-y. Li, B.-g. Sun, S.-w. Zhang, L.-z. Bao, Q.-h. Luo, F. Leach, Y.-z. Zhang, Investigations of combustion characteristics and mechanism of backfire-induced super-knock in a turbocharged hydrogen engine, Energy 312 (2024) 133453.

[17] C. Hong, C. Ji, S. Wang, G. Xin, Y. Qiang, J. Yang, Progressive strategies to avoid and exploit knock limit for optimal performance and stoichiometric operation of a DI hydrogen engine with high CR at WOT conditions, Fuel 357 (2024) 129849. https://doi.org/10.1016/j.fuel.2023.129849

[18] H. Wang, X. Wang, Y. Ge, S. Wang, J. Yang, C. Ji, Analyzing the impact of hydrogen direct injection parameters on flow field and combustion characteristics in wankel rotary engines, Energy 319 (2025) 135004.

[19] R. Novella, A. García, J. Gomez-Soriano, Á. Fogué-Robles, Exploring dilution potential for full load operation of medium duty hydrogen engine for the transport sector, Appl. Energy 349 (2023) 121635. https://doi.org/10.1016/j.apenergy.2023.121635

[20] R. Novella, A. García, J. Gomez-Soriano, Á. Fogué-Robles, Numerical assessment of water injection for improved thermal efficiency and emissions control in a medium-duty hydrogen engine for transportation applications, Fuel 359 (2024) 130455. https://doi.org/10.1016/j.fuel.2023.130455

[21] R. Novella, J. Gomez-Soriano, D. González-Domínguez, O. Olaciregui, Optimizing hydrogen spark-ignition engine performance and pollutants by combining VVT and EGR strategies through numerical simulation, Appl. Energy 376 (2024) 124307. https://doi.org/10.1016/j.apenergy.2024.124307

[22] H. Climent, V. Dolz, B. Pla, D. González-Domínguez, Analysis on the potential of EGR strategy to reduce fuel consumption in hybrid powertrains based on advanced gasoline engines under simulated driving cycle conditions, Energy Convers. Manage. 266 (2022) 115830. https://doi.org/10.1016/j.enconman.2022.115830

[23] J. Serrano, H. Climent, R. Navarro, D. Gonzalez, Methodology to standardize and improve the calibration process of a 1D model of a GTDI engine, SAE Technical Paper 2020-01-1008, 2020, p. 13. https://doi.org/10.4271/2020-01-1008

[24] L. zhi Bao, B. gang Sun, Q. he Luo, Optimal control strategy of the turbocharged direct-injection hydrogen engine to achieve near-zero emissions with large power and high brake thermal efficiency, Fuel 325 (April) (2022) 124913. https://doi.org/10.1016/j.fuel.2022.124913

[25] S. Molina, R. Novella, J. Gomez-Soriano, M. Olcina-Girona, Impact of medium-pressure direct injection in a spark-ignition engine fueled by hydrogen, Fuel 360 (2024) 130618. https://doi.org/10.1016/j.fuel.2023.130618

[26] S. Verhelst, Recent progress in the use of hydrogen as a fuel for internal combustion engines, Int. J. Hydrogen Energy 39 (2) (2014) 1071–1085.

[27] S. Verhelst, J. Vancoillie, K. Naganuma, M. De Paepe, J. Dierickx, Y. Huyghebaert, T. Wallner, Setting a best practice for determining the EGR rate in hydrogen internal combustion engines, Int. J. Hydrogen Energy 38 (5) (2013) 2490–2503. https://doi.org/10.1016/j.ijhydene.2012.11.138

[28] S. Molina, R. Novella, J. Gomez-Soriano, M. Olcina-Girona, Impact of medium-pressure direct injection in a spark-ignition engine fueled by hydrogen, Fuel 360 (PC) (2024) 130618. https://doi.org/10.1016/j.fuel.2023.130618

[29] R. Novella Rosa, J. Gómez Soriano, I. Barbery, G. Alcarria Laserna, Computational analysis of the in-cylinder mixture formation in a direct injection hydrogen spark-ignition engine Int. J. Hydrogen Energy 154 (2025) 150059. https://doi.org/{10.1016/j.ijhydene.2025.150059}.

Glossary

AF_{st}: Stoichiometric Air-fuel Ratio
BTE: Brake Thermal Efficiency
CA10: Combustion after 10% of fuel burnt
CA50: Combustion after 50% of fuel burnt
CA90: Combustion after 90% of fuel burnt
CAD: Crank Angle Degrees
CCV: Cycle-to-Cycle Variation
CFD: Computational Fluid Dynamics
CH_4: Methane
CLD: Cadmium Luminescence Detector
CNG: Compressed Natural Gas
CO_2: Carbon Dioxide
COV_{IMEP}: IMEP covariance
EGR: Exhaust Gas Recirculation
EVC: Exhaust Valve Closing
EVO: Exhaust Valve Opening
EU: European Union
FID: Flame Ionization Detector
GIE: Gross Indicated Efficiency
GHG: Greenhouse Gases
H/C: Hydrogen-Carbon ratio
H_2: Hydrogen
H2-DI: Hydrogen Direct Injection
HC: Hydrocarbons
HCNG: Hydrogen-CNG fuel blends
HICE: Hydrogen Internal combustion Engine
HRR: Heat Release Rate
ICE: Internal Combustion Engine
IMEP: Indicated Mean Effective Pressure

ISCO: Indicated specific CO
ISCO$_2$: Indicated specific CO_2
ISHC: Indicated specific HC
ISNO$_x$: Indicated specific NO_x
IVO: Intake Valve Opening
IVC: Intake Valve Closing
LHV: Lower Heating Value
MBT: Maximum Brake Torque
NDIR: Non-Dispersive Infrared Spectroscopy
NO$_x$: Nitrogen Oxides
O/C: Oxygen-Carbon ratio
O$_2$: Oxygen
OMEx: Oxymethylene Dimethyl Ethers
PFI: Port Fuel Injection
PM: Particulate Matter
PMA: Magneto-Pneumatic Analysis
RON: Research Octane Number
SI: Spark-ignition
SOI: Start of Injection
ST: Spark Timing
TDC: Top Dead Center